

We are IntechOpen, the world's leading publisher of Open Access books Built by scientists, for scientists

6,900

Open access books available

186,000

International authors and editors

200M

Downloads

Our authors are among the

154

Countries delivered to

TOP 1%

most cited scientists

12.2%

Contributors from top 500 universities



WEB OF SCIENCE™

Selection of our books indexed in the Book Citation Index
in Web of Science™ Core Collection (BKCI)

Interested in publishing with us?
Contact book.department@intechopen.com

Numbers displayed above are based on latest data collected.
For more information visit www.intechopen.com



Giant Magnetoimpedance Effect and AC Magnetic Susceptibility in Amorphous Alloys System of FeCoNbBSiCu

Zulia Isabel Caamaño De Ávila,
Amilkar José Orozco Galán and
Andrés Rosales-Rivera

Additional information is available at the end of the chapter

<http://dx.doi.org/10.5772/63024>

Abstract

The study of Giant Magnetoimpedance (GMI) effect of the amorphous alloys system of $\text{Fe}_{72-x}\text{Co}_x\text{Nb}_6\text{B}_{10}\text{Si}_{11}\text{Cu}_1$ (for $x = 35$ and $x = 40$ at. percent Co) and AC magnetic susceptibility for the amorphous alloy of $\text{Fe}_{37}\text{Co}_{35}\text{Nb}_6\text{B}_{11}\text{Si}_{10}\text{Cu}_1$ composition are presented in this chapter. The importance of GMI effect for the improvement of technological applications in sensor devices in amorphous magnetic Fe- and Co-based alloys is introduced; then it is described as the experimental procedure of magnetoimpedance and AC magnetic susceptibility measurements. The obtained results are discussed and finally the conclusions are presented.

Keywords: amorphous, soft magnetic alloys, magnetoimpedance, magnetic susceptibility, amorphous magnetic alloys

1. Introduction

Over the last decades, there has been a growing interest in research on amorphous soft magnetic materials, mainly because they present superior soft magnetic properties, which allowed the development of improved technological applications such as transformer cores, magnetic field sensors, motors, generators, electric vehicles, etc. [1, 2]. The current trend of this kind of materials is their use at high temperatures and high frequencies, for example, in high-frequency power electronics components and power conditioning systems [2].

More recently, the development of high-performance magnetic sensors has promoted the study of interesting magnetic phenomena such as Giant Magnetoimpedance (GMI) and AC Magnetic Susceptibility, in metal-based amorphous alloys.

The Magnetoimpedance (MI) effect has paid more attention in scientific community not only for its applications in sensors devices, especially for low-field detection [3], but also because it has constituted in a useful tool to investigate the magnetism physics.

The MI effect corresponds to the change of the real and imaginary components of electrical impedance $Z = R + iX$ of a ferromagnetic conductor caused by the action of an external static magnetic field [3], being R the Resistance and X the inductance.

The GMI effect consists of large changes in impedance when the materials are subjected to external DC magnetic field and it has been efficiently explained in the terms of classical electrodynamics through the influence of magnetic field on penetration depth of electrical current flowing through the soft magnetic material [4].

The GMI effect is expressed by:

$$\frac{\Delta Z}{Z} = \frac{Z(H) - Z(H_{\max})}{Z(H_{\max})} \times 100 \quad (1)$$

where $Z(H)$ is the impedance of the material in absence of the DC magnetic field and $Z(H_{\max})$ is the impedance at maximum DC field. H_{\max} is usually the external magnetic field sufficient to saturate the impedance [4].

In the case of amorphous ribbon, the skin depth, δ , is given by:

$$\delta = \sqrt{\frac{1}{\pi \mu \sigma f}} \quad (2)$$

where σ is the electrical conductivity, f the frequency of the AC current along the sample, and μ is the transverse permeability of the magnetic ribbon. The DC applied field changes the skin depth through the modification of μ which finally results in a change of the impedance [4].

The GMI effect was investigated for the first time in amorphous ribbons FeCoSiB based on their possible applications in the manufacture of magnetic sensors [5]. Subsequently, it was investigated in $\text{Co}_{70.4}\text{Fe}_{4.6}\text{Si}_{15}\text{B}_{10}$ amorphous ribbons [6] and $\text{Co}_{68.1}\text{Fe}_{4.4}\text{Si}_{12.5}\text{B}_{15}$ amorphous wires [7]. However, in 1994 the GMI effect was discovered in soft magnetic amorphous wires [8]. Since then, there have been numerous studies on the GMI effect in a wide variety of amorphous magnetic alloys in ribbons [1–4, 9–13], wires and microwires [1, 14], and films form [1, 3].

In the same way, AC magnetic susceptibility has been mainly studied for Co-based alloys in wire form [15, 16] and thin films [17]. Also, magnetic susceptibility studies of amorphous and nanocrystalline $\text{Fe}_{44.5}\text{Co}_{44.5}\text{Zr}_7\text{B}_4$ ribbons of 5 cm length and 2 mm width, have been reported

in [18]; however, it has been reported little in the literature about AC magnetic susceptibility in (FeCo)NbBSiCu amorphous alloys.

The magnetic susceptibility is the magnetization degree of a material in response to an applied magnetic field. The susceptibility χ is defined by the following expression:

$$\chi = M / H \quad (3)$$

where M is the magnetization and H is the applied DC magnetic field.

Similarly, AC susceptibility measurement involves an application of a varying magnetic field H_{ac} to a sample.

$$\chi_{AC} = \frac{dM}{dH_{AC}} \quad (4)$$

In the AC measurement, the magnetic moment of the sample is changing in response to an applied AC magnetic field. Therefore, the dynamics of the magnetic system, as the frequency dependence of the complex susceptibility can be studied. Then it is possible to obtain information about relaxation processes and the relaxation times of the magnetic system [19].

The used inductive method for magnetic susceptibility measurements do not need currents or voltages leads; an entire sample volume can be measured and therefore it can provide a volume average of the sample's magnetic response [19]. Hence, inhomogeneous systems as amorphous ribbons can be studied.

The measurement of AC susceptibility can provide important information about AC losses in polycrystalline high-Tc superconductors. In particular, the loss component or imaginary part of the complex susceptibility can be used to probe the nature of the coupling between grains. Also, ac susceptibility can be used to find the transition temperatures of inter- and intergranular regions, as in new granular oxides [19].

GMI and AC magnetic susceptibility are actually opening a new branch of research combining the micromagnetics of soft magnets with the classical electrodynamics.

This chapter presents the results of the GMI effect of amorphous alloys system of $(\text{Fe}_{72-x}\text{Co}_x)\text{Nb}_6\text{B}_{10}\text{Si}_{11}\text{Cu}_1$ (for $x = 35$ and $x = 40$ at. percent Co) and AC magnetic susceptibility for the amorphous alloy of $\text{Fe}_{37}\text{Co}_{35}\text{Nb}_6\text{B}_{11}\text{Si}_{10}\text{Cu}_1$ composition.

2. Experimental procedure

Amorphous ribbons were prepared by the melt-spinning technique. GMI effect measurements of the samples were performed on an electric impedance analyzer equipment, using a frequency range of the current applied from 0.5 to 20 MHz and with a magnetic field applied

parallel to the sample, in a range from -80 to 80 Oe. Amorphous ribbons of 7 cm long and 1.1 mm wide were used for the GMI measurements.

AC magnetic susceptibility measurements were performed on an AC susceptometer, using a frequency range between 10 Hz and 5 kHz and sample lengths between 0.4 and 1 cm, with a constant amplitude of about 1 Vrms. The magnetic field was varied from -74 to 74 Oe. The variation of the external magnetic field (H_{AC}) for each frequency was carried out in three stages: from 0 to 74 Oe, 74 – 74 Oe, and -74 to 74 Oe with a step of 1 Oe.

3. Results and discussion

3.1. Giant magnetoimpedance effect (GMI)

In **Figure 1**, the results of the GMI effect for the alloy of composition $\text{Fe}_{37}\text{Co}_{35}\text{Nb}_6\text{B}_{10}\text{Si}_{11}\text{Cu}_1$ ($x = 35$) are presented. It shows the dependence of the change ratio in total impedance, resistance, and reactance in the frequency range of 0.5 – 20 MHz. It obtains a maximum change ratio of 10.3% for the total impedance, 22.7% for the resistance, and 21.6% for the reactance [13].

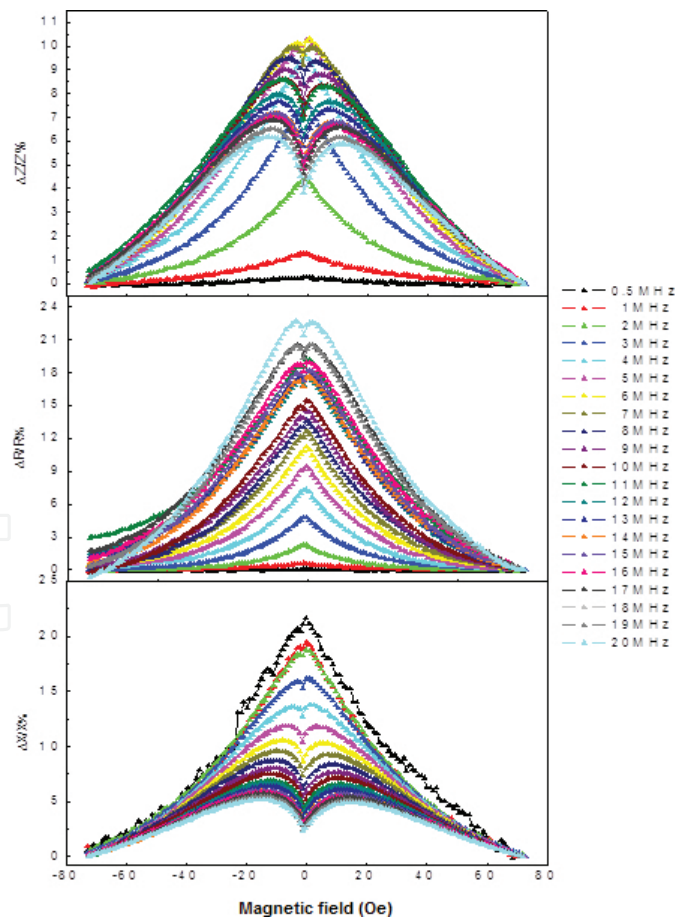


Figure 1. Change ratio in the total impedance $\Delta Z/Z$, the resistance $\Delta R/R$ and in the reactance $\Delta X/X$, as a function of the magnetic field for the amorphous alloy composition $x = 35$ at different frequencies.

The GMI spectra obtained in a frequency range 1–20 MHz for the alloy composition $\text{Fe}_{32}\text{Co}_{40}\text{Nb}_6\text{B}_{11}\text{Si}_{10}\text{Cu}_1$ ($x = 40$) are shown in **Figure 2**.

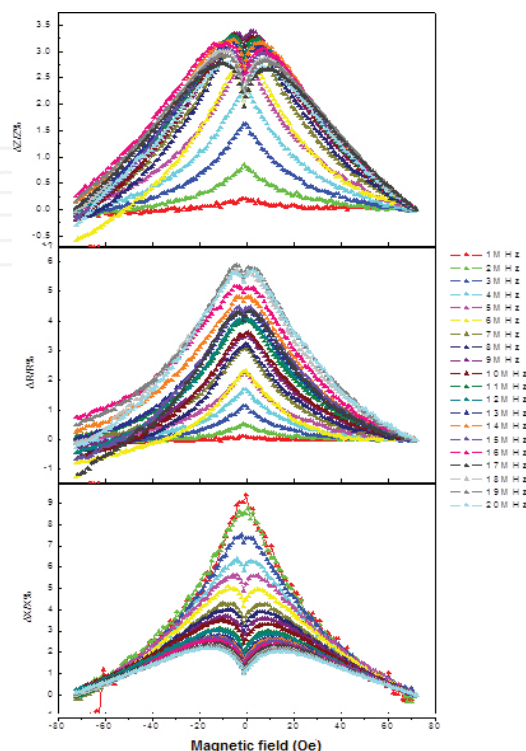


Figure 2. Change ratio in the total impedance $\Delta Z/Z$, the resistance $\Delta R/R$ and the reactance $\Delta X/X$, as a function of the magnetic field for the amorphous alloy composition $x = 40$ at different frequencies [13].

It obtains a maximum change ratio of 3.4% for the total impedance, 5.9% for the resistance, and 9.4% for the reactance [13].

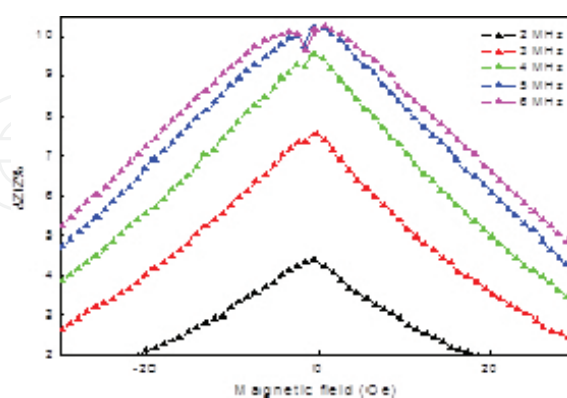


Figure 3. Change ratio of the magnetoimpedance versus magnetic field for the alloy composition $x = 35$ in a frequency range from 2 MHz to 6 MHz.

Figure 3 shows the change MI ratio for frequency range of 2–6 MHz. From the figure, it is observed that the change MI ratio present one peak behavior up to the frequency of 2 MHz;

above this frequency a double peak can be seen. The maximum change MI ratio, $(\Delta Z/Z)_{\max}$, reaches a maximum value in 6 MHz, which is the relaxation frequency, f_x , for this alloy [13].

For the alloy $x = 40$, a double peak is observed above the frequency of 4 MHz, as it can seen in **Figure 4**. The value of the frequency where the maximum change ratio in the magnetoimpedance reaches is 9 MHz; this is the relaxation frequency for this sample [13].

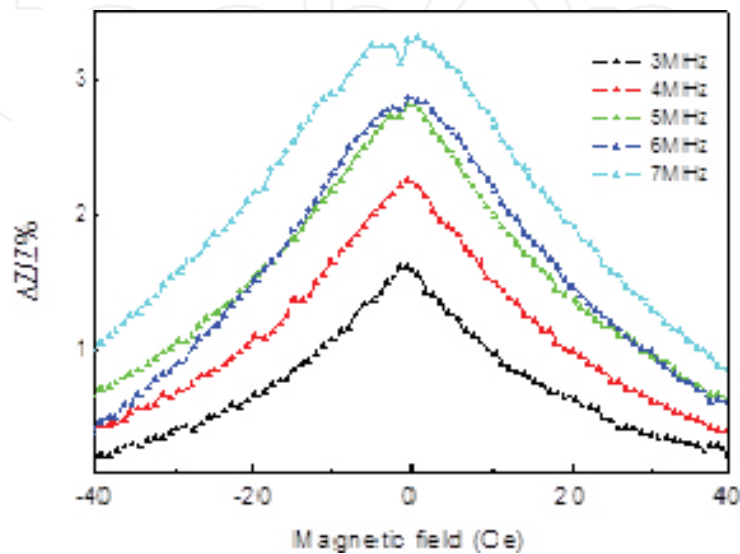


Figure 4. Change ratio of the magnetoimpedance versus magnetic field for the alloy of composition $x = 40$ in a frequency range from 3 MHz to 7 MHz.

The **Table 1** [13] shows the results of the GMI spectra for the alloys of study.

Composition (at. % Co)	$(\Delta Z/Z)_{\max}$ (%)	$(\Delta R/R)_{\max}$ (%)	$(X/X)_{\max}$ (%)	f_x (MHz)
$x = 35$	10.3	22.7	21.7	6
$x = 40$	3.4	5.9	9.4	9

Table 1. Maximum change ratio in the impedance, $(\Delta Z/Z)_{\max}$, in the resistance, $(\Delta R/R)_{\max}$, in the reactance, $(X/X)_{\max}$, and relaxation frequency, f_x , for the amorphous alloys system of $\text{Fe}_{72-x}\text{Co}_x\text{Nb}_6\text{B}_{11}\text{Si}_{10}\text{Cu}_1$.

MI ratio was calculated by the Equation (1):

$$\text{MI ratio} = \frac{\Delta Z}{Z(H_{\max})} \times 100 = \frac{Z(H) - Z(H_{\max})}{Z(H_{\max})} \times 100 \tag{5}$$

where $Z(H)$ is the impedance of the amorphous ribbon in absence of the DC magnetic field and $Z(H_{\max})$ is the impedance at maximum DC field.

The two peak behavior in the spectra of GMI for each composition is due to the rotation of the magnetization produced by the AC current across the ribbon, as it was reported in [12, 20].

The difference between the values of MI for each sample can be due to the modification of the magnetic structure of the material [12], when Fe atoms are substituted by Co atoms, affecting the magnetic permeability and consequently, the impedance of the material.

By the other hand, as it can be seen from the table, the values of the maximum change ratio in the magnetoimpedance for the alloys are very small in comparison with the obtained value (~30%) for the amorphous ribbon of composition $\text{Co}_{64}\text{Fe}_{21}\text{B}_{11}$ reported by Coisson in [21]. Even, it has reported changes in the magnetoimpedance up to 250% for amorphous wires of composition $(\text{Fe}_6\text{Co}_{94})_{72.5}\text{Si}_{12.5}\text{B}_{15}$ [22] and about 50% for amorphous microwires of composition $\text{Fe}_{4.5}\text{Co}_{80}\text{Si}_{10}\text{B}_{1.5}\text{Nb}_4$ [12].

Low values in the percentage change in Z , $(\Delta Z/Z)(\%)$, as a function of H_{dc} at a representative frequency of 2 MHz, were obtained for amorphous ribbons of $\text{Fe}_{68.5}\text{Si}_{18.5}\text{Cu}_1\text{Nb}_3\text{B}_9$ as it was reported by Trilochan Sahoo et al. in [10]. The obtained low values are believed to be related to the magnetostriction effect [10]. The MI effect is also closely related to the magnetic domain structure as well. The domain wall motion contributes to the change in transverse magnetic permeability during the interaction between exciting magnetic field produced by the alternating current flowing across the ribbon axis and the longitudinally applied dc magnetic field. The domain wall motion occurs in different directions and its net effect on transverse permeability is very low. This leads to very low values of $(\Delta Z/Z)$, as it was explained in [10].

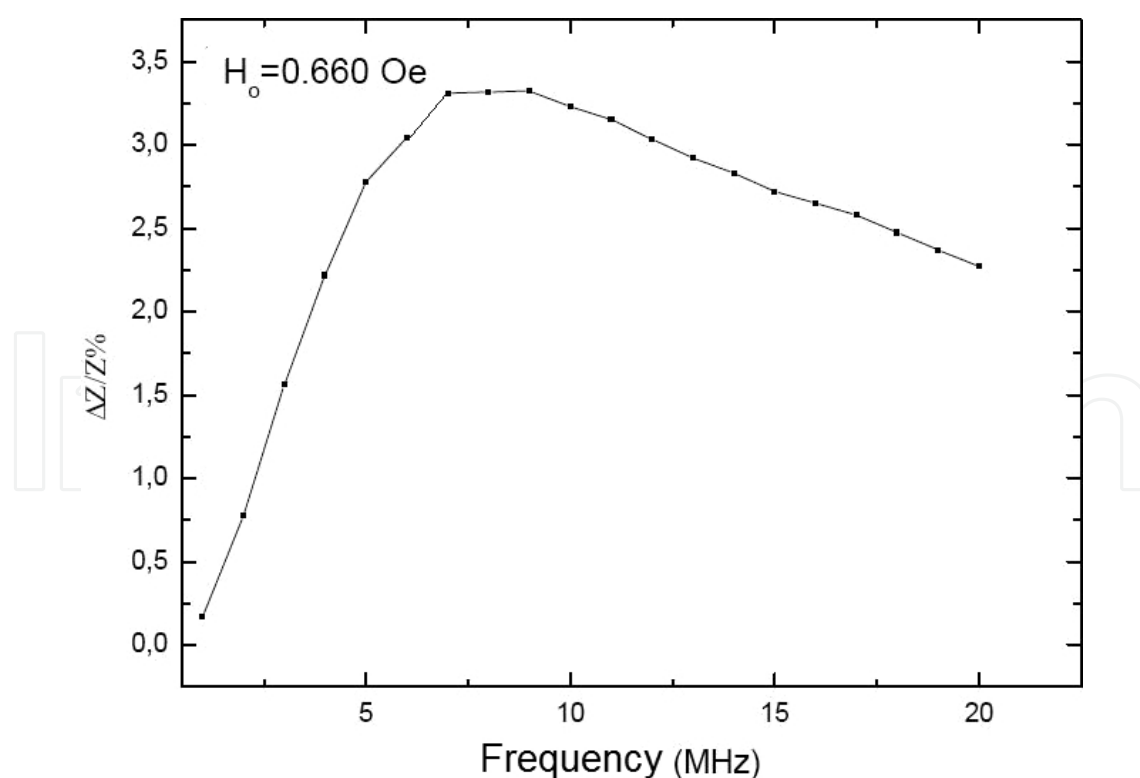


Figure 5. Change ratio of the magnetoimpedance versus frequency for the alloy composition $x = 35$ at DC field $H_c = 0.660$ Oe.

The behavior of the change ratio in the magnetoimpedance as a function of frequency for each alloy composition at constant magnetic field of 0.66 Oe is shown in **Figure 5** and **Figure 6**.

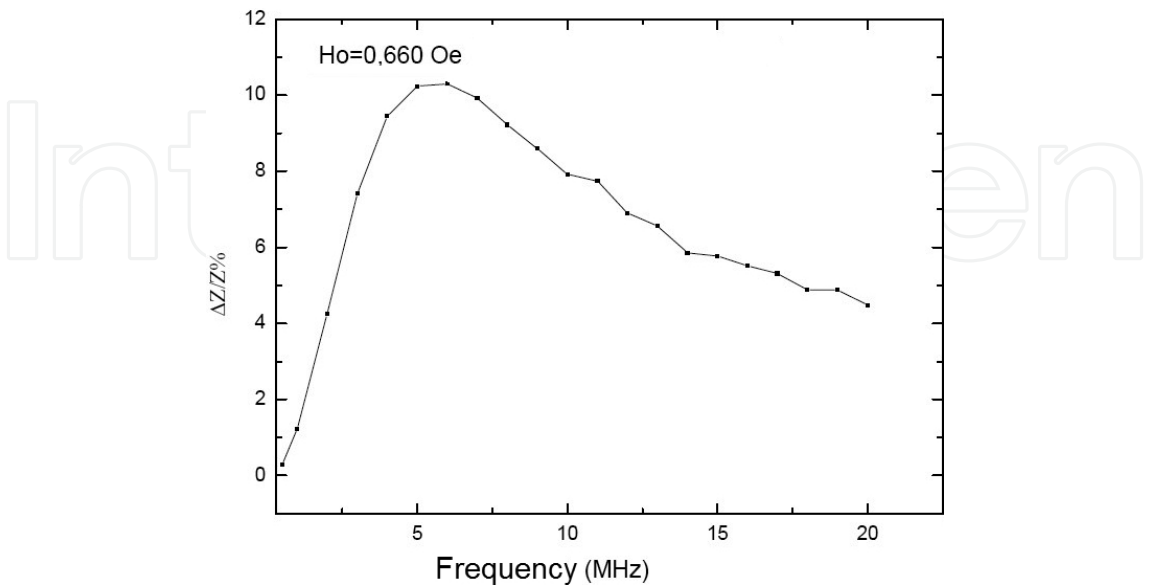


Figure 6. Change ratio of the magnetoimpedance versus frequency for the alloy composition $x = 40$ at DC field $H_c = 0.660$ Oe.

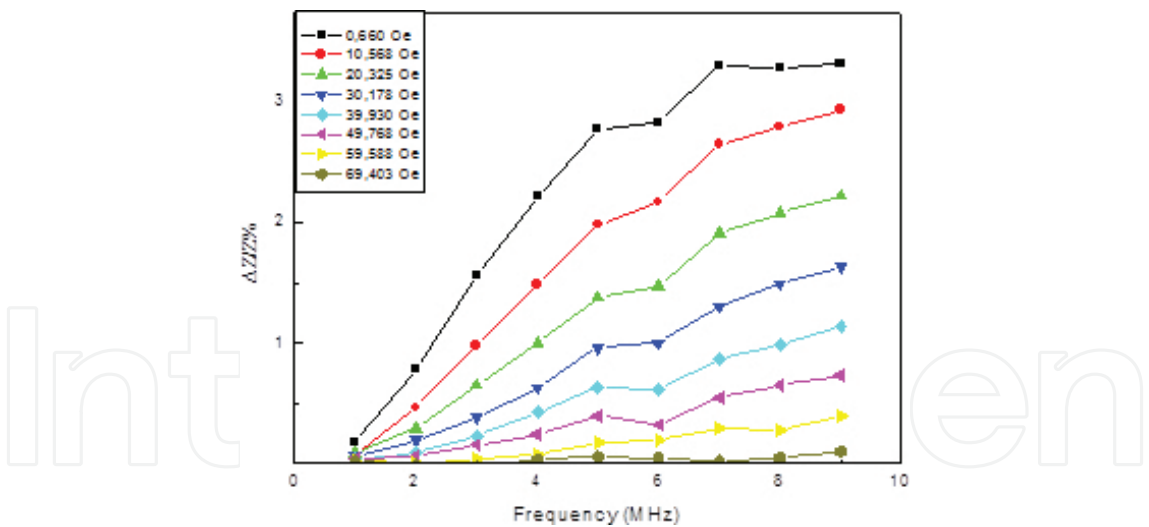


Figure 7. Change ratio of the magnetoimpedance versus frequency for the alloy composition $x = 40$ at DC field from 0.660 Oe until 69.403 Oe.

From these figures, it is observed that the change in the MI increases until to the relaxation frequency corresponding to each composition, and then it diminishes when frequency increases. The increasing in the change MI ratios up to the relaxation frequency is due to the electromagnetic skin effect, as it was reported by Rahman in [23]. However, the decreasing of the change MI ratio above the relaxation frequency is related with the decreasing of the

effective permeability, which is caused by the damping in the movement of the domain walls [12].

Figure 7 illustrates the change MI ratio in the frequency range 1–9 MHz, at constant magnetic fields for the alloy of composition $x = 40$.

It can be noted from the figure that the change ratio of MI decreases when the applied magnetic field is increased in the respective frequencies range. Similar behavior was observed for the alloy composition of $x = 35$ (see **Figure 8**).

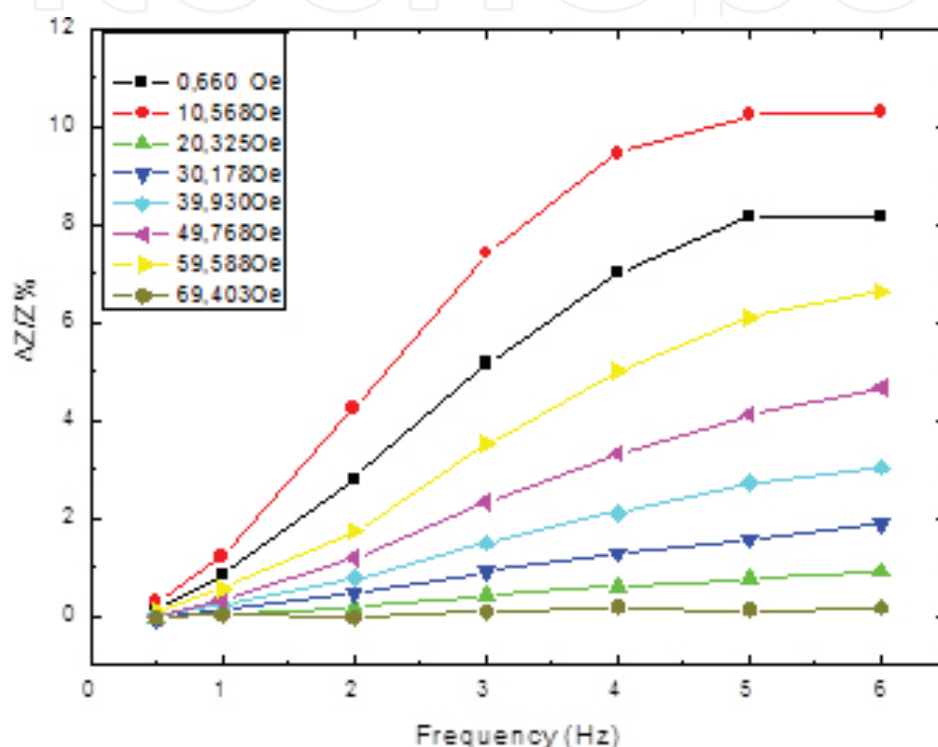


Figure 8. Change ratio of the magnetoimpedance versus frequency for the alloy composition of $x = 35$ at DC field from 0.660 Oe until 69.403 Oe.

3.2. AC Magnetic susceptibility measurements

Figure 9 shows (a) real and imaginary (b) components, χ'_{AC} and χ''_{AC} , of the AC magnetic susceptibility as a function of the applied magnetic field, for the $\text{Fe}_{37}\text{Co}_{35}\text{Nb}_6\text{B}_{11}\text{Si}_{10}\text{Cu}_1$ alloy at a frequency of 40 Hz at room temperature. From the figure, it is observed that the real and imaginary AC susceptibility decreases with increasing magnetic field, both the negative and positive side. A peak at zero magnetic field, corresponding to the maximum value of the AC magnetic susceptibility, is observed.

The continuous decrease of the susceptibility as the magnetic field increase, showing a maximum value at $H = 0$ is the result of the magnetization processes attributed to the domain walls movement, as it was indicated by O. Moscoso [15].

By the other side, the χ''_{AC} imaginary part of the AC magnetic susceptibility, allows to get information about energy losses in magnetization processes. It could be considered that the narrower peak observed in the χ''_{AC} imaginary part is due to the minimum energy loss, which is characteristic of soft magnetic materials and it is associated with the domain walls motion freedom in the material.

The AC magnetic susceptibility dependence on frequency and length of the sample is shown in **Figure 10**. It can be seen that the real AC magnetic susceptibility tends to widen as the frequency increases in **Figure 10(a)**, indicating the strong dependence of AC magnetic susceptibility on frequency, also demonstrating the minimum energy costs in the magnetization processes for this type of system.

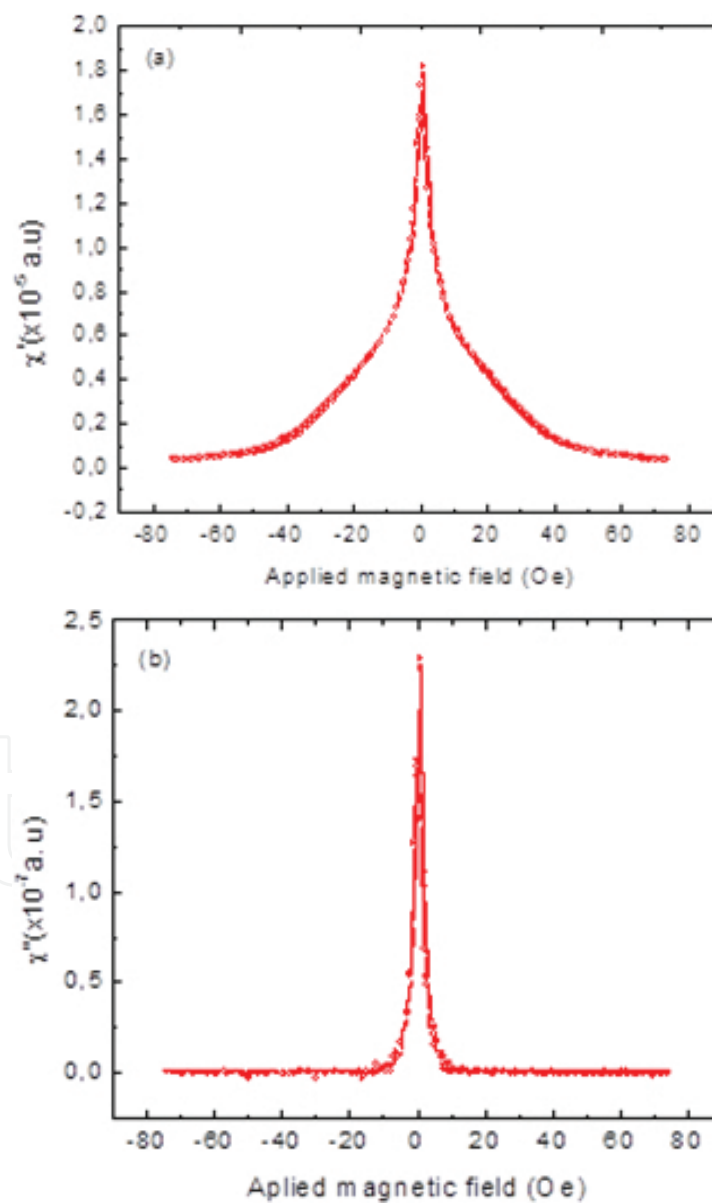


Figure 9. Real AC susceptibility (a) and imaginary AC susceptibility (b) versus applied magnetic field at 40 Hz [24].

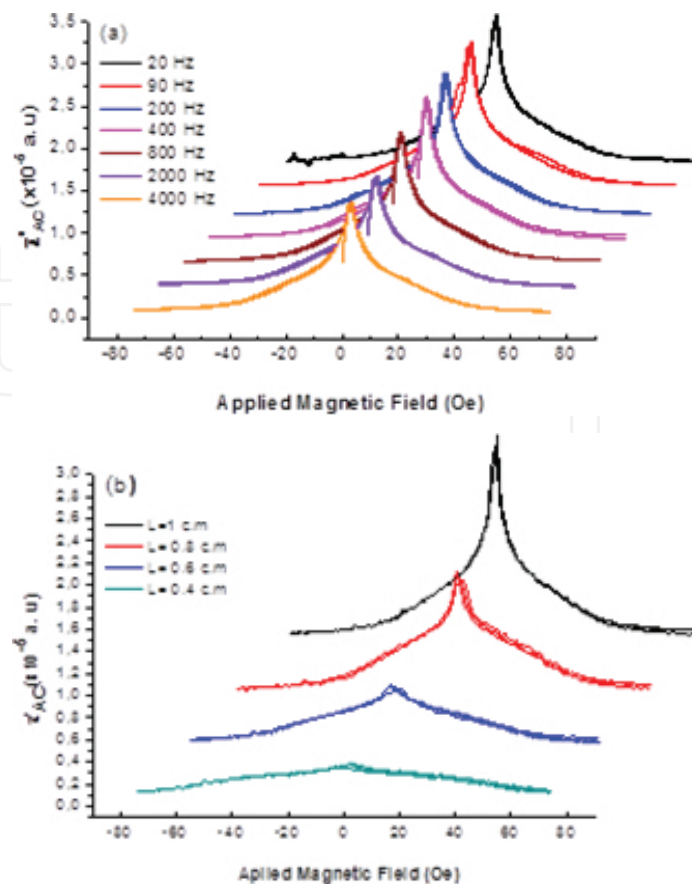


Figure 10. (a) Real part of AC magnetic susceptibility versus external magnetic field at different frequencies and (b) at different lengths of the amorphous alloy of $\text{Fe}_{37}\text{Co}_{35}\text{Nb}_6\text{B}_{11}\text{Si}_{10}\text{Cu}_1$ composition [24].

In **Figure 10(b)** is shown the AC magnetic susceptibility dependence on length of the sample. It can be seen that the AC magnetic susceptibility response enhances as the sample length increases, which is characterized by the emergence of a peak in susceptibility as the length of the sample increases, being more defined for the sample of 1 cm length. This behavior can be due to a possible magnetic hardening of the sample when the length is decreased. The magnetic domain configuration is strongly influenced by the demagnetizing field, because there is an increase in the demagnetization factor along the direction of the sample when the length is reduced; as it was explained by L. Goncalves et al. [16] for alloys of composition $\text{Co}_{70}\text{Fe}_5\text{Si}_{15}\text{B}_{10}$.

4. Conclusions

From the measurements of GMI effect of amorphous alloys system of $\text{Fe}_{72-x}\text{Co}_x\text{Nb}_6\text{B}_{11}\text{Si}_{10}\text{Cu}_1$ ($x = 35$ and 40 at. percent Co) is concluded:

1. The maximum MI ratios obtained for the alloys composition $x = 35$ and $x = 40$ were 10.3% and 3.4%, respectively. The difference between the values obtained can be attributed to the change in the magnetic structure of the material, when replacing Fe by Co, which affects the magnetic permeability and consequently the impedance of the material.

2. The studied amorphous ribbons does not present a “giant” MI effect as the present soft magnetic amorphous alloys such as Finemet- and Co-based alloys reported in literature.
3. The dependence of the MI ratios with the frequency and the applied magnetic field is mainly due to electromagnetic skin effect for low and intermediate frequencies.

From measurements of AC magnetic susceptibility of $\text{Fe}_{37}\text{Co}_{35}\text{Nb}_6\text{B}_{11}\text{Si}_{10}\text{Cu}_1$ amorphous alloy it is concluded that AC magnetic susceptibility depends strongly on the frequency and length of the sample and its response is closely related to a minimum energy loss, which is characteristic for this type of alloys.

Acknowledgements

To the group of Physics of Materials II of the Universidad Autónoma de Barcelona (Bellaterra, Spain), for the collaboration in the preparation of the samples by the melt-spinning technique.

To Universidad del Atlántico (Barranquilla, Colombia) for financial support for the internship of A. Orozco at the Universidad Nacional de Colombia, in Manizales, for AC magnetic susceptibility measurements.

The first author highly appreciates MSc. L. Costa Arzuza for his collaboration in some of the results of GMI effect.

Author details

Zulia Isabel Caamaño De Ávila^{1*}, Amilkar José Orozco Galán¹ and Andrés Rosales-Rivera²

*Address all correspondence to: zuliacaamano@mail.uniatlantico.edu.co

1 Physics Department, Basics Sciences Faculty, Universidad del Atlántico, Barranquilla, Colombia

2 Magnetism and Advanced Materials Laboratory, Exact Sciences and Natural Faculty, Universidad Nacional de Colombia, sede Manizales, Manizales, Colombia

References

- [1] Rajat Roy K, Ashis Panda K and Amitava M. In: Ahmad Z, editor. New Trends in Alloy Development, Characterization and Application. Intech (Croatia); 2015. pp. 39–60. DOI: 10.5772/60772.

- [2] Škorvánek I, Marcin J, Capik M, Varga M, Kováč J, Janotova I, Švec P, Idzikowski B. Soft Magnetic Melt-spun Ribbons for Energy and Sensor Applications. *Acta Electro-technica et Informatica*. 2013; 1:45–48. DOI: 10.2478/aei-2013-0009.
- [3] Silva E, Da Silva R, Gamino M, De Andrade A, Vázquez M, Corrêa M, Bohn F. Asymmetric magnetoimpedance effect in ferromagnetic multilayered biphasic films. *J. Magn. Magn. Mater.* 2015; 393:260–264.
- [4] Wei Lu, Yewen Xu, Jindan Shi, Yiming Song, Xiang Li. Soft magnetic properties and giant magnetoimpedance effect in thermally annealed amorphous $\text{Co}_{68}\text{Fe}_4\text{Cr}_3\text{Si}_{15}\text{B}_{10}$ alloy ribbons. *J. Alloys Compd.* 2015; 638:233–238.
- [5] Makhotkin V, Shurukhin B, Lopatin V, Marchukov Y, Levin Y. A magnetic field sensor based on rotating amorphous ribbons. *Sens. Actuators A*. 1992; 31:220–222.
- [6] Machado F, Lopes da Silva B, Montarroyos E. Magnetoresistance of the random anisotropic $\text{Co}_{70.4}\text{Fe}_{4.6}\text{Si}_{15}\text{B}_{10}$ alloy. *J. Appl. Phys.* 1993; 73:6387. DOI: 10.1063/1.352659.
- [7] Mandal K and Ghatak S. Large magnetoresistance in an amorphous $\text{Co}_{68.1}\text{Fe}_{4.4}\text{Si}_{12.5}\text{B}_{15}$ ferromagnetic wire. *Phys. Rev. B*. 1993; 47:14233.
- [8] Panina L and Mohri K. Magneto-impedance effect in amorphous wires. *Appl. Phys. Lett.* 1994; 65:1189.
- [9] Béron F, Valenzuela L, Knobel M, Melo L, Pirota K. Hysteretic giant magnetoimpedance effect analyzed by first-order reversal curves. *J. Magn. Magn. Mater.* 2012; 324:1601–1605.
- [10] Trilochan Sahoo, Majumdar B, Srinivas V, Srinivas M, Nath T, Agarwal G. Improved magnetoimpedance and mechanical properties on nanocrystallization of amorphous $\text{Fe}_{68.5}\text{Si}_{18.5}\text{Cu}_1\text{Nb}_3\text{B}_9$ ribbons. *J. Magn. Magn. Mater.* 2013; 343:13–20.
- [11] Ganesh Kotagiri and Markandeyulu G. Magnetoimpedance studies on as-quenched $\text{Fe}_{66-x}\text{Co}_x\text{Ni}_7\text{Si}_7\text{B}_{20}$ ($x=0, 33$ and 66) ribbons. *Physica B*. 2014; 448:20–23.
- [12] Rosales-Rivera A., Valencia, V. H, Pineda-Gómez P. Three-peak behavior in giant magnetoimpedance effect in $\text{Fe}_{73.5-x}\text{Cr}_x\text{Nb}_3\text{Cu}_1\text{Si}_{13.5}\text{B}_9$ amorphous ribbons. *Physica B*. 2007; 398:252–255.
- [13] Caamaño Z, Costa L, Rosales A. Giant Magnetoimpedance effect and magnetization in amorphous alloys system of FeCoNbBSiCu. *Rev. Mex. Fis. S.* 2012; 58:35–38.
- [14] Zhukov A, Ipatov M, Blanco J.M, Zhukova V. GMI Effect of Ultra-Soft Magnetic Soft Amorphous Microwires. *Open Mater Sci J.* 2012; 6:39–43.
- [15] Rosales-Rivera A, Moscoso-Londoño O, Muraca D. Magnetization dynamics and magnetic hardening in amorphous FeBSi alloys. *Rev. Mex. Fis. S.* 2012; 58:155–159.
- [16] Goncalves L, Soares J, Machado F, De Azebedo W. *Physica B*. 2006; 384:152–154.

- [17] Chen Yuan-Tsung, Hsieh W.H. Thermal, magnetic, electric, and adhesive properties of amorphous $\text{Co}_{60}\text{Fe}_{20}\text{B}_{20}$ thin films. *J. Alloys Compd.* 2013; 552:283–288.
- [18] Varga M, Varga R, Komova E, Csach K, Vojtanik P. Temperature evolution of magnetic susceptibility during devitrification of Cu-free HITPERM alloy. *J. Magn. Magn. Mater.* 2010; 322:2758-2761.
- [19] Nikolo M. Superconductivity: A guide to alternating current susceptibility measurements and alternating current susceptometer design. *Am. J. Phys.* 1995; 63:57–61.
- [20] Vázquez M, Kurlyandskaya G, Garcia-Benitez J, Sinnecker J. *IEEE Trans. Magn.* 1999; 35:3358–3360.
- [21] Coisson M, Kane S, Tiberto P, Vinai F. Influence of DC Joule-heating treatment on magnetoimpedance effect in amorphous $\text{Co}_{64}\text{Fe}_{21}\text{B}_{15}$ alloy. *J. Magn. Magn. Mater.* 2004; 271:312–317.
- [22] Pal S, Manik N, Mitra A. Dependence of frequency and amplitude of the ac current on the GMI properties of Co based amorphous wires. *Mater. Sci. Eng. A.* 2006; 415:195–201.
- [23] Rahman Z, Kamruzzaman M, Rahman M. A. *J. Mater. Process. Technol.* 2004; 153–154:791–796.
- [24] Orozco A, Caamaño Z, Rosales A. AC magnetic susceptibility and influence of heat treatment on obtaining the nanocrystalline structure for the amorphous alloy of $\text{Fe}_{37}\text{Co}_{35}\text{Nb}_6\text{B}_{11}\text{Si}_{10}\text{Cu}_1$ composition. *JPCS.* 2016; 687:1–4. DOI:10.1088/1742-6596/012109.